The Observation of Tungsten Unresolved Transition Arrays Spectra at High Electron Temperature in Experimental Advanced Superconducting Tokamak (EAST) Plasma[*)]

Yunxin CHENG[1)], Ling ZHANG[1,a)], Shigeru MORITA[2)], Ailan HU[1)], Chengxi ZHOU[1)], Darío MITNIK[3)], Wenmin ZHANG[1,4)], Fengling ZHANG[1,4)], Jiuyang MA[1,4)], Zhengwei LI[1,5)], Yiming CAO[1,5)] and Haiqing LIU[1)]

[1)]*Institute of plasma physics, Chinese Academy of Sciences, Hefei 230031, China*
[2)]*National Institute for Fusion Science, Toki, Gifu 509-5292, Japan*
[3)]*Instituto de Astronomía y Física del Espacio (CONICET-Universidad de Buenos Aires), Buenos Aires 1428, Argentina*
[4)]*University of Science and Technology of China, Hefei 230026, China*
[5)]*Anhui University, Hefei 230601, China*

(Received 31 July 2024 / Accepted 15 October 2024)

To optimize the plasma performance of fusion devices using tungsten plasma-facing components (PFCs), it is crucial to study the transport of tungsten impurities. This work focuses on the observation of line emissions from various charge states of tungsten ions in high-temperature plasmas utilizing Extreme Ultraviolet (EUV) spectrometers. Line emissions from W^{26+}-W^{32+} ions are observed in the 45-55 Å band at electron temperatures below 2.0 keV, while line emissions from W^{34+}-W^{45+} ions appear in the 55-70 Å band at electron temperatures above 3.0 keV. Additionally, radial profiles of W-UTA spectra in plasma with different electron temperature show that as the electron temperature decreases from 5.0 keV to 3.0 keV, the peak position of W^{26+}-W^{32+}ions move inward from ρ~0.5 to ρ~0.2. The line intensity profiles of W^{42+}-W^{45+} ions accumulate within a narrow region of plasma core, specifically at $\rho < 0.4$. This study provides essential experimental data to support further research on tungsten impurity transport, control of tungsten content, and the enhancement of plasma performance.

Keywords: EAST tokamak, high temperature plasma, impurity ion, extreme ultraviolet spectroscopy, tungsten spectra

DOI: 10.1585/pfr.20.2402010

1. Introduction

In magnetic-confinement tokamak fusion devices with D-T long pulse discharges, high-Z tungsten material is a unique candidate for plasma facing components (PFCs) due to several optimal characteristics, including a high sputtering threshold, and high neutron resistance [1]. Tungsten materials are currently used in several tokamak devices, such as ASDEX Upgrade [2], JET [3], and WEST [4]. In ITER, tungsten material was also chosen for the first wall and divertor. To increase the heat and particle exhaust capability of divertor plate, the upper and lower divertors of EAST were upgraded to tungsten divertor in 2014 and 2021, respectively. However, the plasma-wall interaction inevitably leads to tungsten ions entering the plasma. The incompletely ionized tungsten impurity ions enhance radiation loss, which seriously degrades confinement of the high-performance plasma, potentially leading to discharge termination. Studying tungsten impurity transport and controlling tungsten content in plasma is crucial for fusion devices using tungsten PFCs. Extreme ultraviolet (EUV) spectroscopy in the wavelength range of 10-500 Å is exceedingly important for diagnosing tungsten impurity ions, because most line emissions useful for impurity diagnostics exist in this range, as observed in WEST [5] and LHD [6]. In this work, the line emissions from different charge state tungsten ions are observed by fast-time response EUV spectrometer in plasma of varying temperatures, and the tungsten spectra profiles with temperature variations are analyzed through a space-resolved EUV spectrometer.

2. EUV Spectrometers on EAST

Passive spectroscopy is a unique tool for studying the detailed behavior of tungsten ions in fusion plasmas, including their temporal evolution and spatial distribution. Sets of EUV spectrometer systems have been developed in EAST to observe the tungsten impurity ion line emissions from the plasma edge to core [7–11]. In this study,

[a)] *Corresponding author's e-mail: zhangling@ipp.ac.cn*

[*)] This article is based on the presentation at the 26th International Conference on Spectral Line Shapes (ICSLS2024).

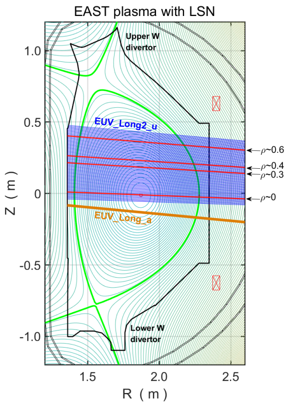

Fig. 1 Poloidal cross section of EAST tokamak (last closed flux surface: thick green line) and lines of sight (LOS) of fast-time-response EUV spectrometer (EUV_Long_a: brown line) and space-resolved EUV spectrometer (EUV_Long2_u: blue lines). The lines of sight that are tangent to the magnetic surface with normalized radius of ρ~0 (plasma center), ρ~0.3, ρ~0.4, and ρ~0.6 are indicated by solid red lines.

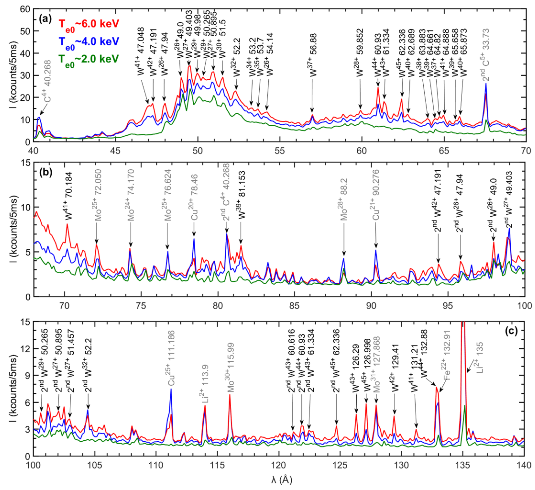

Fig. 2 EUV spectra at (a) 40-70 Å, (b) 68-100 Å and (b) 100-140 Å measured by the 'EUV_Long_a' spectrometer in the plasma with electron temperature of 2.0 keV (green), 4.0 keV (blue), 6.0 keV (red).

a space-resolved EUV spectrometer with a spatial resolution of ΔZ=2.5 cm, named 'EUV_Long2_u', is utilized to measure the intensity profile of tungsten ion line emissions. A fast-time response EUV spectrometer with a temporal resolution of 5 ms/frame, named 'EUV_Long_a', observes the temporal evolution of tungsten unresolved transition arrays (UTA) spectra. Figure 1 shows the lines of sight of these two EUV spectrometers, and the lines of sight that are tangent to the magnetic surface with normalized radius of ρ~0 (plasma center), ρ~0.3, ρ~0.4, and ρ~0.6 are indicated by solid red lines. The number of lines of sight for EUV_Long2_u is 64.

3. Tungsten UTA Spectra in High Temperature Plasma

Figure 2 shows the tungsten spectra measured by the 'EUV_Long_a' spectrometer in plasma with electron temperatures (T_{e0}) of 2.0 keV, 4.0 keV, and 6.0 keV. The wavelengths denoted in the figure are taken from National Institute of Standards and Technology (NIST) database [12]. The tungsten unresolved transition arrays (W-UTA) can be observed in the wavelength range of 45-70 Å, composed of line emissions from W^{26+}-W^{45+} ions. When the electron temperature does not exceed 2.0 keV, only the line emissions from low-charge tungsten ions can be measured in the 45-55 Å band, e.g., W^{26+} at 49.0 Å, W^{27+} at 49.403 Å, W^{29+} at 49.98 Å, W^{29+} at 50.265 Å, W^{30+} at 51.5 Å, and W^{32+} at 52.2 Å. The line emissions from medium- and highly-charged tungsten ions can be observed in the 55-70 Å band in plasma with electron temperatures of 4.0 keV and 6.0 keV, e.g., W^{37+} at 64.82 Å, W^{39+} at 65.658 Å, W^{40+} at 65.873 Å, W^{41+} at 64.888 Å, W^{43+} at 61.334 Å, W^{44+} at 60.93 Å, and W^{45+} at 62.336 Å. If the intensity of first-order spectral lines is strong, their second-order spectra can be observed in the longer wavelength range of 90-140 Å, e.g., 2nd W^{26+} at 49.0 Å, 2*nd* W^{32+} at 52.2 Å, 2nd W^{43+} at 60.93 Å, and 2*nd* W^{45+} at 62.336 Å. These second order spectral lines can be utilized for wavelength calibration. Furthermore, some isolated lines from highly-charged tungsten ions appear in the 125-135 Å band, e.g., W^{41+} at 131.21 Å, W^{42+} at 129.41 Å, W^{43+} at 126.29 Å, W^{44+} at 132.88 Å, and W^{45+} at 126.998 Å. Based on these spectral lines from neighboring charge states of tungsten ions, it is possible to compute the transport coefficients of tungsten ions in all charge states when combined with the STRAHL transport code. Therefore, these isolated lines from highly-charged tungsten ions are crucial for studying tungsten impurity transport in fusion devices.

4. Tungsten UTA Spectra Intensity Profile in Different Electron Temperature Plasma

Figure 3 displays the image of W-UTA spectra observed by a space-resolved EUV spectrometer, as well as the spectra in the 45-70 Å band from different plasma locations. The electron temperature (T_{e0}) and density (n_{e0}) in the plasma center are 5.0 keV and 2.3×10^{19} m^{-3}, respectively. The peak position of the intensity profile for line emissions in the 45-55 Å band, predominantly from W^{26+}-W^{30+} ions, is located at ρ~0.3-0.5. The line emissions from W^{37+}-W^{45+} ions appeared in higher-temperature plasma core, i.e., in the vicinity of $\rho < 0.3$.

Figure 3 (b) shows the four spectra observed at different normalized radii of plasma with varying electron temperatures. The selection of normalized radii and cor-

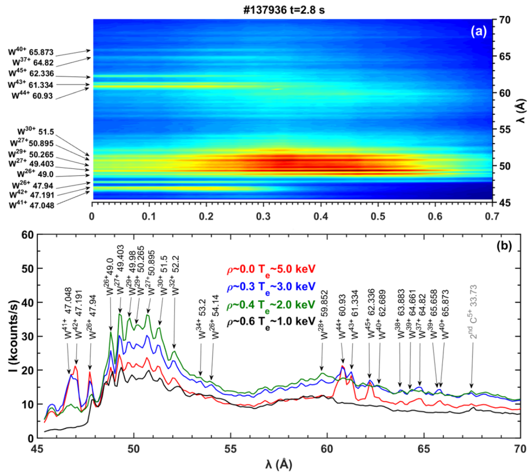

Fig. 3 (a) The spectra image and (b) the W-UTA spectra at different plasma locations in wavelength of 45-70 Å observed by space-resolved EUV spectrometer at H-mode plasma with NBI and ECRH heating (T_{e0} = 5.0 keV and n_{e0} = 2.3 × 10^{19} m^{-3}). Each W line is identified as denoted in the figure. The ρ is the normalized radius, ρ = 0 means the plasma core.

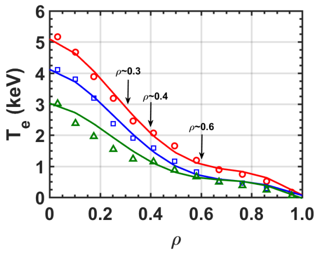

Fig. 4 Radial profile of electron temperature measured by heterodyne radiometer system. The selection of plasma location corresponding the observation of W-UTA spectra in Fig. 3 (b) are denoted with black arrows.

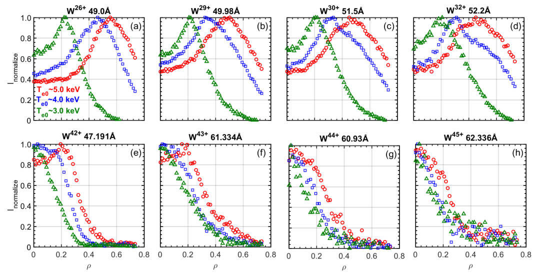

Fig. 5 The normalized radial profile of the chord line-integrated intensity of (a) W^{26+} at 49.0 Å, (b) W^{29+} at 49.98 Å, (c) W^{30+} at 51.5 Å, (d) W^{32+} at 52.2 Å, (e) W^{42+} 47.191, (f) W^{43+} at 61.334 Å, (g) W^{44+} at 60.93 Å, (h) W^{45+} at 62.336 Å observed by space-resolved EUV spectrometer in NBI and ECRH heated H-mode plasma with core electron temperature (T_{e0}) of 3.0 keV (green open triangles), 4.0 keV (blue open circles), 5.0 keV (red open squares), respectively.

responding electron temperature are indicated in Fig. 4 by black arrows and red solid line, respectively. The electron temperature profile is measured by the heterodyne radiometer system [13]. The shape of W-UTA spectral lines changes significantly with variations in electron temperature. The spectral lines of W^{41+} at 47.048 Å, W^{42+} at 47.191 Å, W^{43+} at 61.334 Å, W^{44+} at 60.93 Å, and W^{45+} at 62.336 Å appear with substantial intensity in the plasma core where T_{e0} is 5.0 keV. At ρ~0.3 with T_e of 3.0 keV, the line intensity of W^{43+} at 61.334 Å, W^{44+} at 60.93 Å, and W^{45+} at 62.336 Å decrease significantly, while the lines of W^{41+} at 47.048 Å and W^{42+} at 47.191 Å still maintain certain intensity. These spectral lines from high-charge tungsten ions, i.e., W^{37+}-W^{45+}, cannot be observed at ρ~0.4 where T_e = 2.0 keV. Conversely, the intensity of line emissions from low-charge tungsten ions, e.g., W^{26+}-W^{32+}, increases as the temperature decreases. At ρ~0.6 where T_e = 1.0 keV, the overall intensity of W-UTA spectra decreases, and only the lines of W^{26+}-W^{32+} are observed.

Figure 5 presents the normalized line intensity profiles of W^{26+} at 49.0 Å, W^{29+} at 49.98 Å, W^{30+} at 51.5 Å, (d) W^{32+} at 52.2 Å, W^{42+} at 47.191, W^{43+} at 61.334 Å, W^{44+} at 60.93 Å, and W^{45+} at 62.336 Å in H-mode plasma at different electron temperatures. To accurately calculate the intensity of the overlapping spectral lines in UTA, it is necessary to perform a Gaussian fitting on the line shape to effectively distinguish them from the overlapping spectral lines. The corresponding electron temperature profiles are illustrated in Fig. 4. The profiles indicate that the distribution of W^{42+}-W^{45+} ions is more peaked compared to W^{26+}-W^{32+} ions, which is attributed to the higher ionization energy of the high-charged tungsten ions. As the core electron temperature (T_{e0}) decrease from 5.0 keV to 4.0 keV, the peak position of W^{26+}, W^{29+}, W^{30+}, W^{32+} move inward from ρ~0.5 to ρ~0.2, and the profiles of W^{30+} and W^{32+} change from a hollow to a peaked distribution. When T_{e0} is further reduced to 3.0 keV, the peak positions in the profiles of W^{26+}, W^{29+}, W^{30+}, W^{32+} shift inward to ρ~0.2. Additionally, the line intensity profiles of W^{42+}-W^{45+} ions accumulate within a narrower region in the plasma core, i.e., in the vicinity of $\rho < 0.3$. The observations of tungsten spectra in the plasma with varying electron temperatures offer significant data support for further studies on tungsten impurity transport.

5. Summary

Line emissions from different charge states of tungsten ions are observed by EUV spectrometers in the plasma with varying electron temperatures. The W-UTA at 45-70 Å is composed of line emissions from W^{26+}-W^{45+} ions, and the UTA composition varies with electron temperature. When the electron temperature does not exceed 2.0 keV, only line emissions from W^{26+}-W^{32+} ions can be measured in the 45-55 Å band. Line emissions from W^{34+}-W^{45+} ions can be observed in the 55-70 Å band in plasma with electron temperatures higher than 3.0 keV. Comparative analyses of tungsten impurity profiles at different temperatures reveal that the distribution of high-charge tungsten ions is more peaked. Additionally, as the electron temperature decreases, the peak position in the profiles of W^{26+}, W^{29+}, W^{30+}, and W^{32+} move inward from $\rho\sim0.5$ to $\rho\sim0.2$, and the line intensity profiles of W^{42+}-W^{45+} ions accumulate within a narrower region in the plasma core. This study provides essential experimental data to support further research on tungsten impurity transport, control of tungsten content, and the enhancement of plasma performance.

Acknowledgments

This work was supported by the National Magnetic Confinement Fusion Energy R&D Program of China (Grant Nos. 2022YFE03180400, 2022YFE03020004), National Natural Science Foundation of China (Grant No. 12322512), and Chinese Academy of Sciences President's International Fellowship Initiative (PIFI) (Grant Nos. 2020VMA0001, 2024PVA0074).

[1] J. Roth *et al*., J. Nucl. Mater. **390-391**, 1-9 (2009).
[2] R. Neu *et al*., Plasma Phys. Control. Fusion **49**, B59 (2007).
[3] G. Matthews *et al*., Phys. Scr. **T145,** 014001 (2011).
[4] J. Bucalossi *et al*., Fusion Eng. Des. **89**, 907 (2014).
[5] R. Guirlet *et al*., Plasma Phys. Control. Fusion **64**, 105024 (2022).
[6] T. Oishi *et al*., Nucl. Fusion **64**, 106011 (2024).
[7] L. Zhang *et al*., Nucl. Instrum. Meth. A **916**, 169 (2019).
[8] L. Zhang *et al*., Rev. Sci. Instrum. **86**, 123509 (2015).
[9] Z. Xu *et al*., Nucl. Instrum. Meth. A **1010**, 165545 (2021).
[10] Y. Cheng *et al*., Rev. Sci. Instrum. **93**, 123501 (2022).
[11] Y. Cheng *et al*., Nucl. Instrum. Meth. A **1057**, 168714 (2023).
[12] A.E. Kramida *et al*., 2023 National Institute of Standards and Technology (NIST) NIST Atomic Spectra Database (Version5.11).
[13] H. Zhao *et al*., Rev. Sci. Instrum. **89**, 10H111 (2018).